7.1. Introduction

The ceramic materials with good thermal stability and high dielectric constant have attracted significant attention particular their applications in microelectronic devices, memory and capacitors. Recently, a temperature independent dielectric constant has been observed in $Bi_3Ti_4O_2$ (BTO) and $CaCu_3Ti_4O_{12}$ (CCTO) compounds. $Bi_3Ti_4O_2$ shows high Curie temperature (T_c = 675 °C) and low dielectric constant, which makes it significant for multiple applications such as memory chips, optical displays, and piezoelectric converters of pyroelectric devices in a wide temperature range from 200 to 600 °C and used in transducers, capacitors, sensors **[**Siriprapa *et al.* (2009), Trubnikov *et al.* (2009)]. The pitch of electric properties by compositional conversion as well as the shape and size effect can meet important description for Curie temperature, coercivity, conductivity, compliance, etc. **[**Moure *et al.* (2009), Villegas *et al.* (2009)]. It gives a potential pertinence as an applicable candidate for high temperature piezoelectric property. In addition, BTO is an enthralling material of lead-free and environmental eco-friendly in nature. The Bi-layer structure was described an Aurivillius family to have the general formula $(Bi_2O_2)^{+2}$ – $(A_{m-1}B_mO_{3m+1})^{-2}$, where A is Bi, Pb, Sr, Ba, K, Ca, or Na; B is Nb, Ti, Mo, W, Fe, or Ta. The Bi-layered perovskite oxide such as BTO, $SrBi_2Nb_2O_9$ (SBN) or $SrBi_2Ta_2O_9$ (SBT) has been developed, because of the fatigue free in nature of Lanthanum substituted bismuth titanate, $Bi_3LaTi_3O_{12}$. A Bi-layered perovskite oxide with a platinum electrode has received increasing consideration on ferroelectric applications, such as nonvolatile random access memory **[**Desu *et al.* (1995), Park *et al.* (1999)]. A fatigue-free ferroelectric material such as $SrBi_2Nb_2O_9$ (SBN) and $SrBi_2Ta_2O_9$ (SBT), which is always a Bi-layered perovskite oxide, $Bi_3LaTi_3O_{12}$ has many tempting properties i;e large values of remnant polarization and low processing temperature which make it more suitable for Si-based integrated circuit (IC) technology. $CaCu_3Ti_4O_{12}$ compounds explained a compositional formula of $ACu_3Ti_4O_{12}$ have a great interest in recent years, because of its abnormal and bewitching dielectric properties [Fang *et al.* (2004), Prakash *et al.* (2007), Prakash *et al.* (2006), Hao *et al.* (2009)]. CCTO exhibits an extremely large frequency dielectric constant ~10^4 at room temperature, which is nearly constant over a wide temperature range from 100 to 600 K. Since CCTO has been promising among the large number of perovskite oxides, Most of the literatures, CCTO have been published and retouch its dielectric properties, particularly minimize the dielectric losses by cationic substitutions with different metal ions, using different of synthesis routes. On the other hand, $Bi_{2/3}Cu_3Ti_4O_{12}$ (BCTO) is an entertaining material that is structurally similar to CCTO type oxide having high dielectric constant [Liu *et al.* (2004), Liu *et al.* (2005), Ferrarelli *et al.* (2006)]. However, A-site vacancies make it different from others analogous oxides. The particles analysis, morphology and compositional homogeneity were shows good strength of electrical and dielectric properties of ceramic.

In the present work composite containing BCTO and BLTO materials of lanthanum-substituted bismuth having composition 0.1 $Bi_{2/3}Cu_3Ti_4O_{12}$ - 0.9 $Bi_{4-x}La_xTi_3O_{12}$ (BCLT-19) was synthesized by semi-wet route and studied it dielectric and magnetic behavior.

7.2. Experimental

The composite 0.1 $Bi_{2/3}Cu_3Ti_4O_{12}$ - 0.9 $Bi_3LaTi_3O_{12}$, (BCLT-19) was prepared by the mixing of individual materials of $Bi_{2/3}Cu_3Ti_4O_{12}$ and $Bi_3LaTi_3O_{12}$ obtained by semi-wet route and using bismuth nitrate, $Bi(NO_3)_3.5H_2O$ (99.5%; Merck) solid lanthanum oxide, La_2O_3 (99.0%; Merck) copper nitrate, $Cu(NO_3)_2.3H_2O$ (99.8%; Merck) and titanium oxide,

TiO_2 (99.9%; Merck) were taken as starting materials. A stoichiometric amount of bismuth nitrate and copper nitrate were prepared by using deionized water and mixed together in a beaker. The citric acid, $C_6H_8O_7.H_2O$ (99.5%; Merck) and calculated amount of solid TiO_2 were added to the solution. The solution was heated on a magnetic stirrer at 70 - 80 °C. After evaporation, the water, resulting precursor powder of $Bi_{2/3}Cu_3Ti_4O_{12}$ was calcined at 800 °C for 6 h in the muffle furnace. The synthesis process of $Bi_3LaTi_3O_{12}$ ceramic was same as $Bi_{2/3}Cu_3Ti_4O_{12}$. For making composite a calculated amount of calcined powder of $Bi_{2/3}Cu_3Ti_4O_{12}$ and $Bi_3LaTi_3O_{12}$ were taken and mixed each other with the help of ethanol and ground for 12 h. The resulting composite material was used to make pellets on applying 4-5 tons of pressure using poly vinyl alcohol as a binder. The pellets were preheated to 500 °C for 2 h to remove the binder and finally sintered at 900 ºC for 8 h.

The confirmation of phase formation was identified by X-ray diffractometer (Rigaku miniflex 600, Japan) with Cu-K_{α}, radiation at scanning rate of 1-2°/min. The particle size was observed by a transmission electron microscope (TEM, FEI TECANI G^2 20 TWIN, USA). The sample for TEM analysis was prepared in acetone using ultrasonication. The suspensions of BCLT-19 composite was added on the carbon-coated copper grid and dried for 4 h in hot air oven at 60 °C. The microstructure of the composite was explained by a scanning electron microscope (ZEISS, model EVO-18 research; Germany). The elemental analysis of BCLT-19 composite was carried by EDX (Oxford instrument; USA). The surface roughness and morphology of composite were determined by atomic force microscopy (NTEGRA Prima, Germany). The magnetic measurement of composite was carried out by using a Quantum Design MPMS-3, (Magnetic property Measurement System) over a wide temperature 2–300 K and applied magnetic field of 7 tesla. The function of temperature for zero field cooled

(ZFC) and field cooled (FC) magnetization at 100 Oe applied field were carried out using SQUID VSM dc magnetometer. The dielectric properties of the BCLT-19 composite were measured by LCR meter (PSM 1735, Numetri Q 4thLtd. U.K.) with variation of temperature (300 - 500 K) and frequency (100 Hz - 5 MHz).

7.3. Results and discussion

7.3.1. Microstructural studies

The X-Ray diffraction pattern of BCLT-19 composite powder calcined at 800 °C for 8 h and pallet sintered at 900 °C for 8 h is illustrated in Fig. 7.1 All the peaks match each other and show the phase formation of $Bi_{2/3}Cu_3Ti_4O_{12}$ and $Bi_3LaTi_3O_{12}$ (JCPDS card no. 80-1343 and 50-0278). The crystallite size (D) of the BCLT-19 composite was determined by the line broadening method.

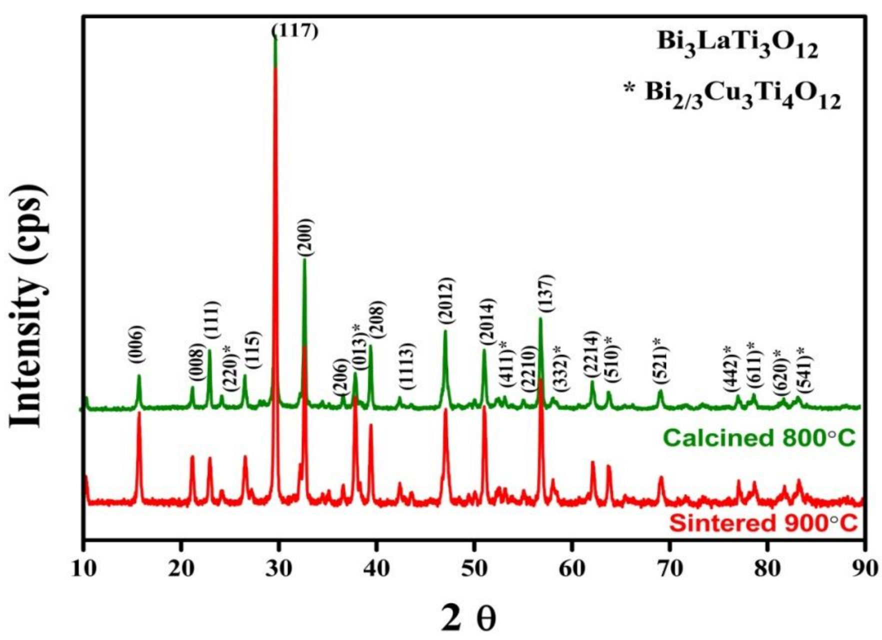

Fig.7.1. XRD patterns of BCLT-19 composite (a) calcined at 800 °C for 6 h and (b) sintered at 900 °C for 8 h.

In the single-line analysis method, the Cauchy component of the Voigt function exhibited crystallite size given by Scherrer formula, as shown in equation [Gautam *et al.* (2017)].

$$D = k\lambda/\beta \cos\theta \qquad (7.1)$$

where k is a crystal shape coefficient (k = 0.89), β is the full width at half maximum (FWHM), λ is the wavelength of X-ray, θ is the diffraction angle of the peaks. The average crystallite size of BCLT-19 composite was calculated by using the formula and found to be 44 nm. Fig.7.2 shows the FT-IR spectrum of BCLT-19 composite of dry powder and calcined powder at 800 °C for 6 h. The peak 1633 cm^{-1} observed in dry powder shows the OH vibrational mode of the absorbed water molecule [Ocwelwang *et al.* (2014)].

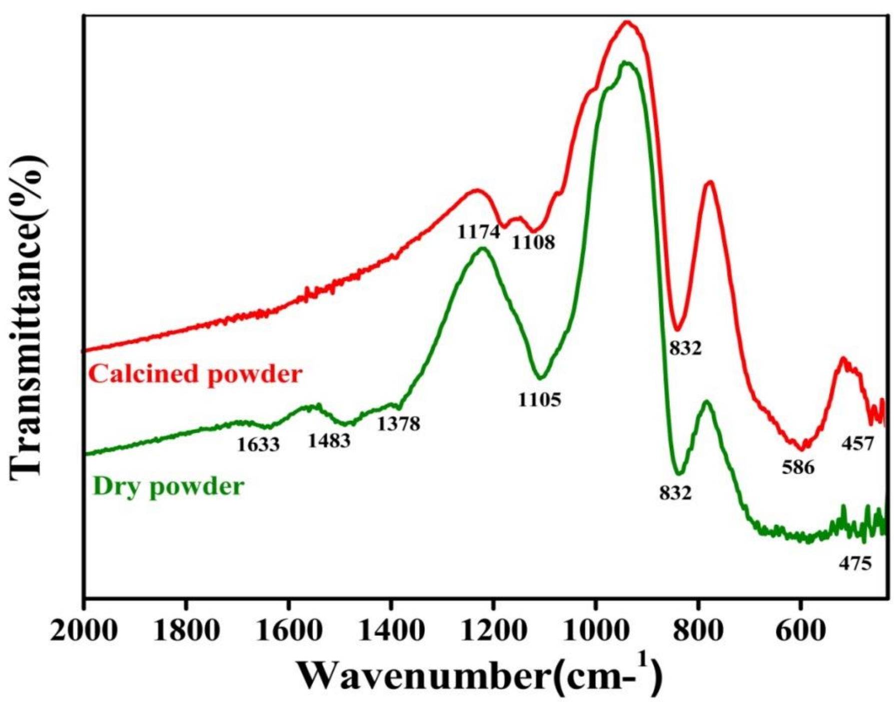

Fig.7.2. FITR spectra for the BCLT-19 composite (a) dry powder (b) calcined at 800 °C for 6 h.

The peaks in the 1483- 1100 cm^{-1} frequency region for dry and calcined powder are attributed to the nitrate bands. The peak observed in low frequency region 454, 475, 586, and 832 cm^{-1} for dry and calcined powder were indicate to the Ti-O-Ti, Ti-O band Cu-O stretching vibration **[**Tachikawa *et al.* (1997)]**.** Oxygen–metal bonds were shown in the 400–840 cm^{-1} [Simoes *et al.* (2006), He *et al.* (2006)]. Fig.7.3 exhibited low magnification TEM image of BCLT-19 composite sintered at 900 °C for 8 h.

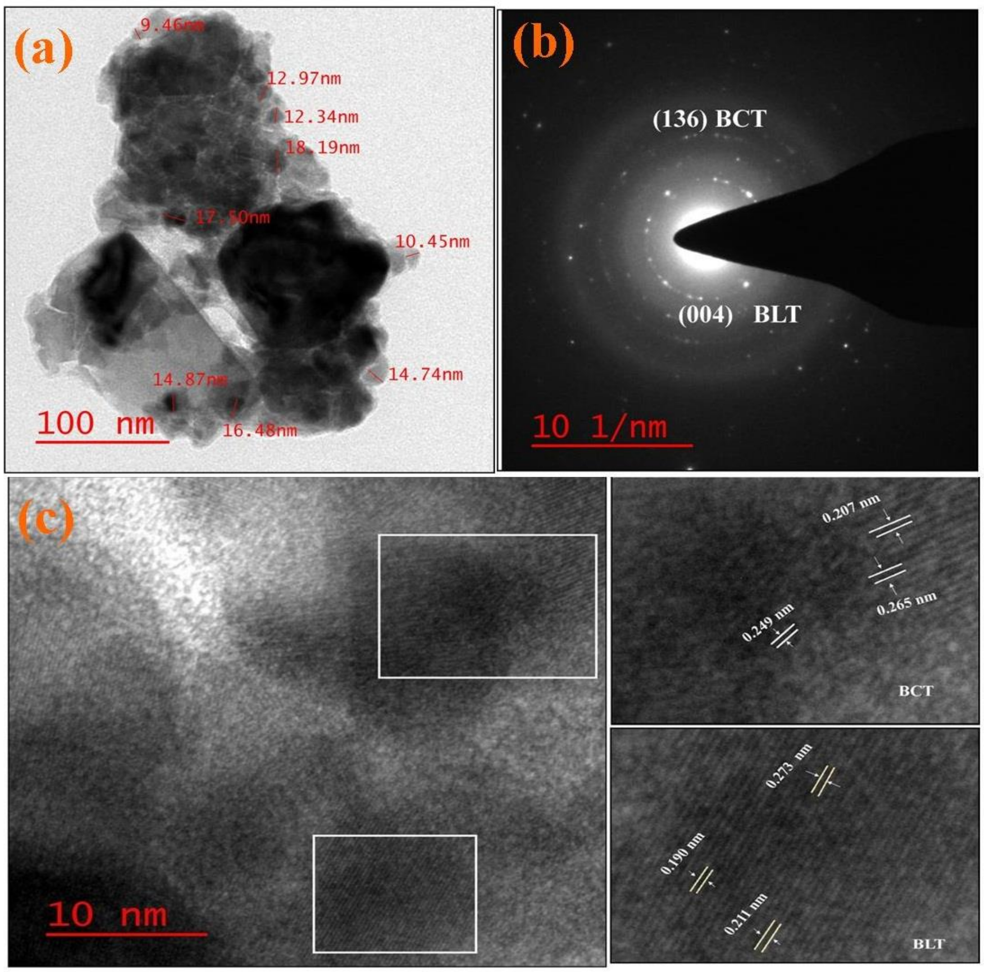

Fig.7.3. (a) shows TEM micrographs of BCLT-19 composite sintered at 900 °C for 8 h, (b) SAED pattern (c) presents a high resolution TEM micrograph of the BCLT-19 composite.

The nano particle of composite was exhibited to heterogeneous shape and size. The average particle size of the composite was found to be 14 ± 5 nm. Figure shows the agglomeration of particle. TEM and XRD analysis confirms the formation of nano composite. Fig.7.3(b) shows the SAED (selected area electron diffraction) pattern of BCLT-19 composite. The presence of diffraction rings also supporting the formation of nano composite.

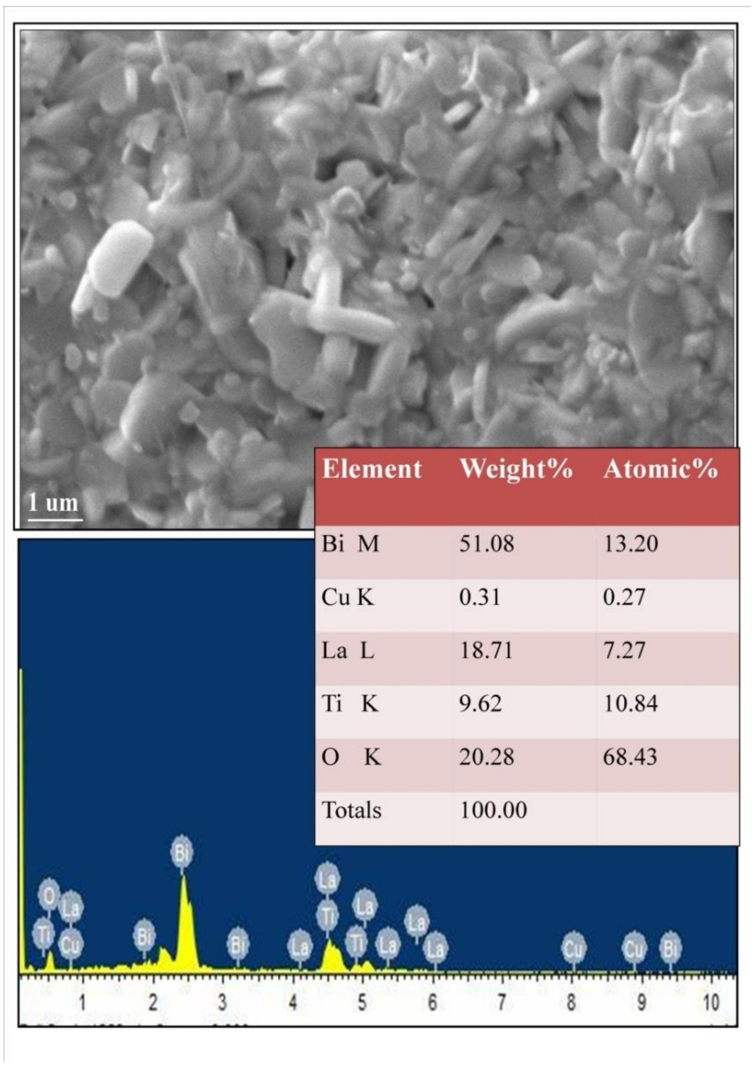

Element	Weight%	Atomic%
Bi M	51.08	13.20
Cu K	0.31	0.27
La L	18.71	7.27
Ti K	9.62	10.84
O K	20.28	68.43
Totals	100.00	

Fig.7.4. (a) SEM micrograph and (b) EDX spectrum of BCLT-19 composite sintered at 900 °C for 8 h.

Fig.7.3(c) shows the high-resolution TEM analysis (HR-TEM) of BCLT-19 nano composite. In HR-TEM image two distinct parallel lines have occurred at two different marked places which indicate inter-planer distance (d) between two parallel lines. The values of d were found to be 0.273, 0.190, 0.211 nm for BLTO and 0.249, 0.265, 0.207 nm for BCTO. The d values were matched with the planes (200), (2012), (1113) for BLTO ceramic and 0.244, 0.265, 0.207 for BCTO ceramic respectively in the composite. The results supported by XRD data. The scanning electron micrograph (SEM) and elemental analysis of BCLT-19 composite sintered at 900 °C for 8 h is shown in Fig.7.4. Tubular and spherical and heterogeneous structure of grains was exhibited in SEM image (fig.a). The confirmation of elemental composition and the atomic percentage of BCLT-19 composite were shown in Fig.7.4(b). The atomic percentage data was obtained by EDX studies. Bi, La, Cu, Ti and O elements in the composites were found to be 13.20, 7.27, 0.27, 10.84 and 68.43, confirmed purity of the materials. AFM analysis of composite was explained in Fig.7.5(a-d). Fig.7.5(a) shows the watershed image which clearly indicate the presence of grain and grain boundary in the composite. Fig.7.5(b) shows three-dimensional picture of the composite from which the root means square roughness, average roughness and maximum area peak height, were found to be 233.637, 50.615 and 68.391 nm respectively. Root mean square roughness was the square root of the broadcasting of surface height and ponders to be more sentient than the average roughness for large divergence from the mean line and also apply in computing the kurtosis and skew parameters. The average roughness was the mean height as calculated over the thorough measured area or length. Maximum peak to height was the high of the highest peak of the composite calculated from mean line of the surface.

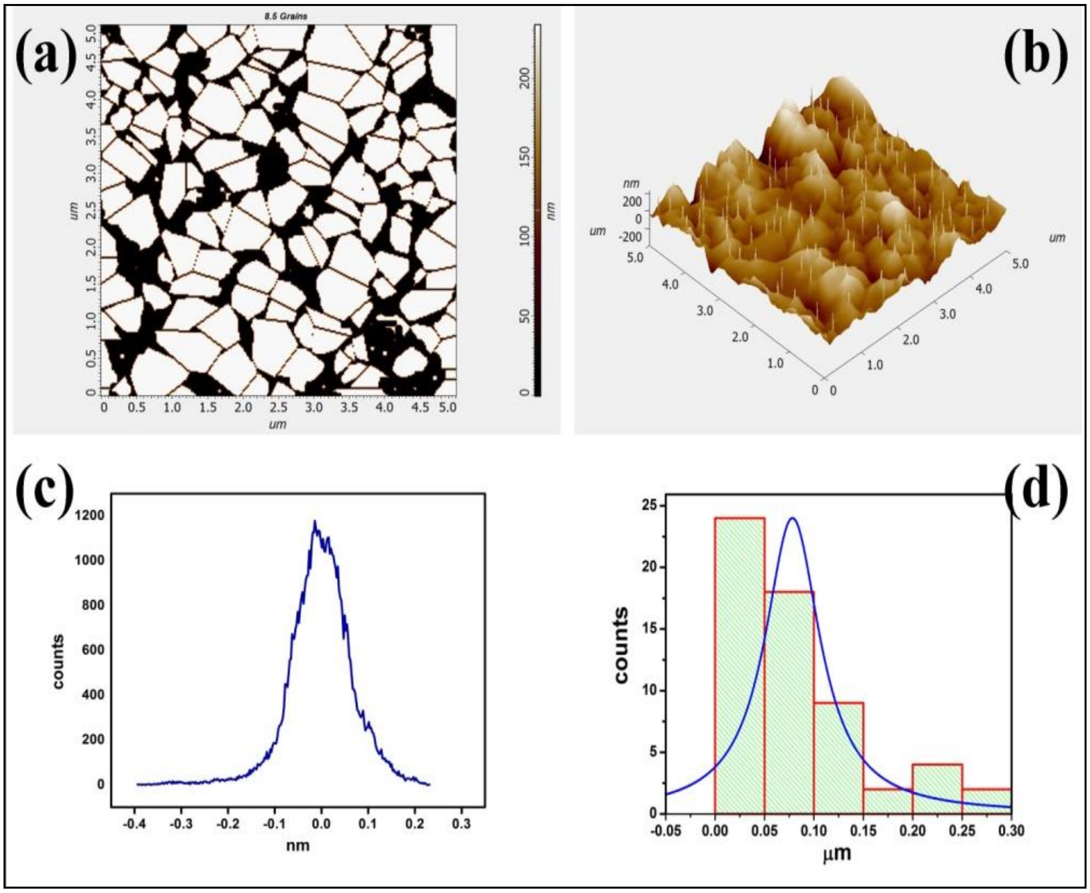

Fig.7.5. (a) watershed image of two-dimensional AFM image showing grains and grain-boundaries, (b) three-dimensional image and (c&d) histogram curve shows roughness of particle and average grain size for the composite BCLT-19 sintered at 900 °C for 8h.

The results of root means square roughness, average roughness and maximum area peak height, determined by the grain size of composite and depend on sintering temperature [Kumar et al. (2012]. The histogram plots derived from the corresponding three dimensional image shown in Fig. 7.5(c&d). The total roughness of the composite may be seen from Fig. 7.5(c). The average grain size of the composite was calculated from Fig. 7.5(d). The average grains size was found to be 19 nm out of 139 grains.

7.3.2 Magnetic Properties

The magnetic behavior of BCLT-19 composite was determined by zero field cooled and field cooled curve in the temperature range 2-300 K with applied magnetic field 100 Oe shown in Fig. 7.6(a).

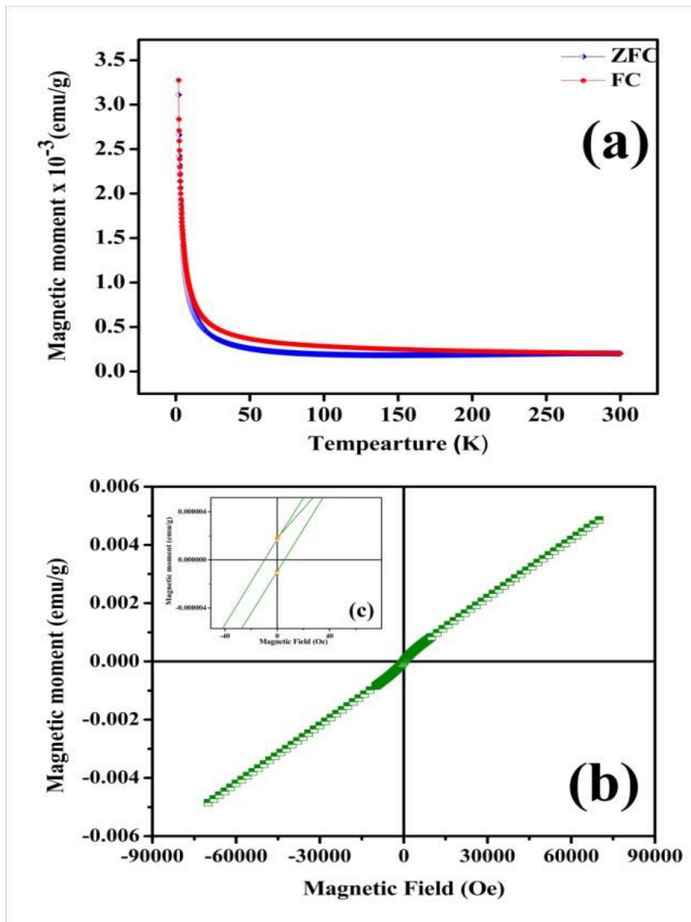

Fig.7.6.(a) Temperature-dependent zero field cooled (ZFC) and field cooled (FC) magnetization measured at H=100 Oe, (b) magnetization versus applied field at 300 K for the BCLT-19 composite.

The ZFC and FC curve were bifurcated at 235 K and merged at 7 K with 0.967×10^{-3} emu/g magnetic moment. The changes in the curve may indicate magnetic transition anti ferromagnetic to weak ferromagnetic [Pomiro *et al.* (2017), Zhang *et al.* (2015)]. Fig.7.6(b) shows the hysteresis loop, magnetization with magnetic field (H) measured at 7 T for the composite. The curves show weak saturation magnetization and it was stable at room temperature. It shows weak ferromagnetic in nature [Gautam *et al.* (2017)]. The inset figure shows open hysteresis loop, it explained the coercivity of composite. The coercivity was found to be 26 Oe. This observation explains the hard magnetic nature of the composite.

7.3.3 Dielectric studies

Fig.7.7 shows the variation of the dielectric constant (ε') and tangent loss (tan δ) with temperature at few selected frequencies (100 Hz, 1 kHz, 10 kHz and 100 kHz). The dielectric constant (ε') was increased with increasing temperature (300-500 K) at low frequency (100 Hz). The value of dielectric constant BCLT-19 composite was found to be 3147, 2715, 1855 and 1547 at 100 Hz, 1 kHz, 10 kHz and 100 kHz respectively; at 503 K. the high value of dielectric constant may be explain due to the presence of chemical micro-heterogeneities and space charge polarization in the composite. The plot of temperature dependence tan δ of the BCLT-19 composite was shown in Fig.7.7(b).

The value of tan δ was largely depending on low temperature and low frequency region. The low value of tan δ was found to be 2.6, 0.9, 0.2 and 0.1 at 100 Hz, 1 kHz, 10 kHz and 100 kHz at 500 K, respectively. The value of high dielectric loss was due to the presence of high conductivity nature in the composite. Fig.7.8 shows the variations of dielectric constant (ε') and tangent loss (tan δ) with frequency at few selected temperature. The dielectric constant and tangent loss increased with low frequency. The dielectric constant and

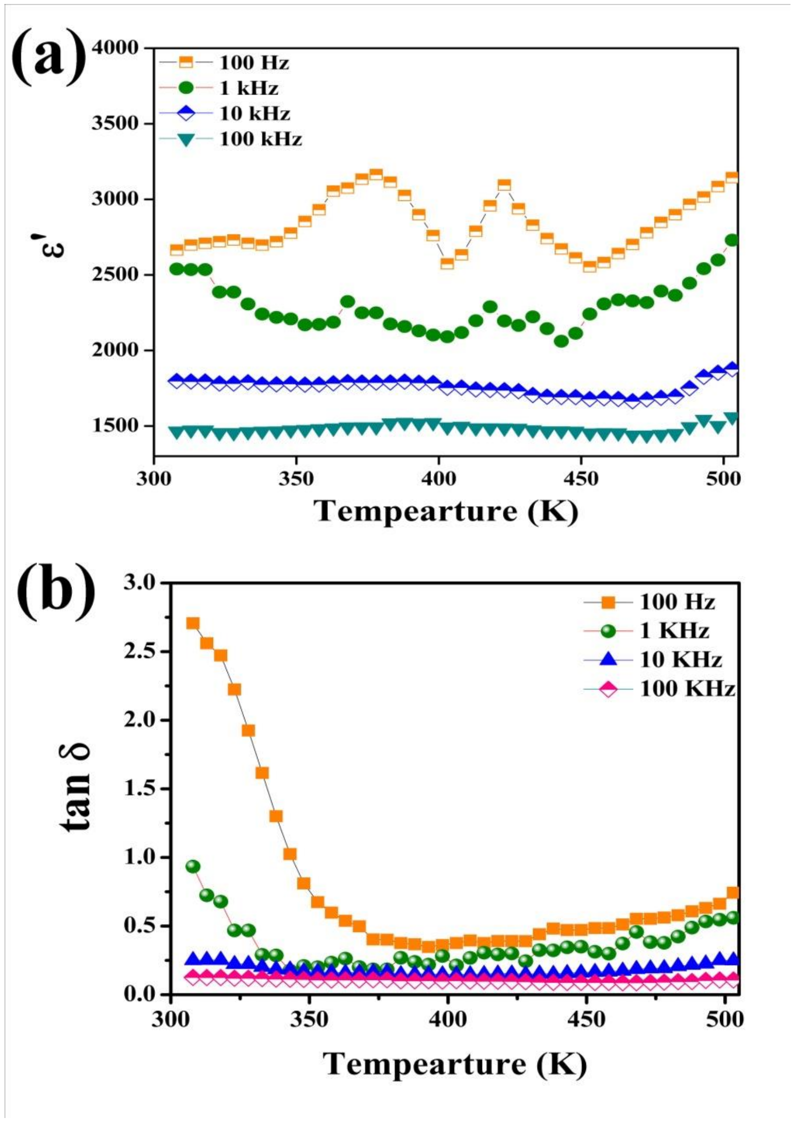

Fig.7.7. Plot of (a) dielectric constant and (b) tangent loss (tan δ) as a function of temperature for BCLT-19 composite sintered at 900 °C for 8 h.

tangent loss at low frequency are high due to the presence of space charge .polarization which arises accumulation of charge carriers at the interface of semi-conducting grains and insulating grain boundary. The value of dielectric constant and tangent loss were found to be at low frequency (~10^2 Hz) 1897 and 2.8 at 503 K respectively [Singh *et al.* (2014)].

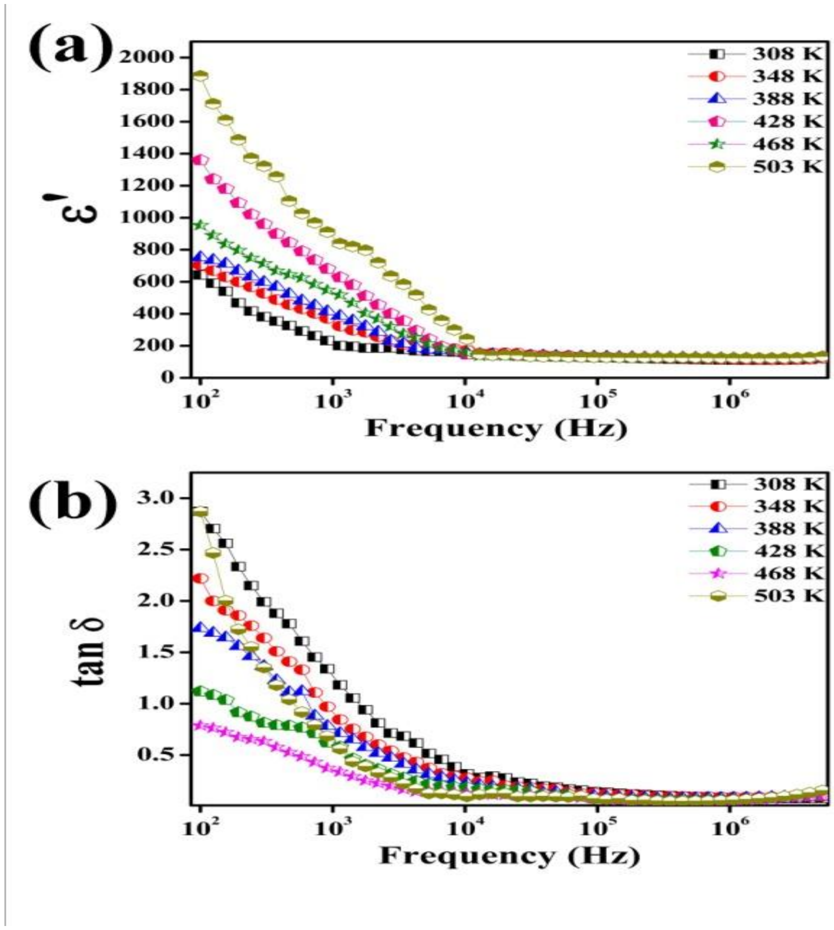

Fig.7.8. Plot of (a) dielectric constant and (b) tangent loss (tan δ) as a function of frequency for BCLT-19 composite at few selected temperatures.

7.4. Conclusion

A new composite materials $0.1Bi_{2/3}Cu_3Ti_4O_{12}$ - 0.9 $Bi_3LaTi_3O_{12}$ (BCLT-19) has been synthesized by semi-wet route using metal nitrate solution and solid TiO_2 powder. The phase formation of the BCLT-19 composite was confirmed by XRD. Oxygen–metal bonds were confirmed by FT-IR in the frequency range at 400–840 cm^{-1}. The particle size was found to be 14 ± 5 nm by TEM analysis. EDX spectrum confirms the presence of elemental composition of composite, which confirms the purity of composite. The value of root means square roughness, average roughness and maximum area peak height were found to be 233.637, 50.615 and 68.391 nm respectively, and average grains size found to be 19 nm from AFM analysis. The result was supported by TEM analysis. The M-T and M-H curve were exhibited magnetic transition anti-ferromagnetic to weak ferromagnetic in nature of the composite. The value of dielectric constant (ε') is 3147 at 100 Hz and 503 K. the result, shows nano composite BCLT-19 a good dielectric constant and temperature dependent at low frequency due to space charge polarization.